

A contact probe using Michelson interferometers for CMMs

Chao-Min Huang^{*a}, Bo-Hsun Liao^a, Kuang-Chao Fan^a

^aNational Taiwan University, No.1, Sec. 4, Roosevelt Road, Taipei, Taiwan 106

*r99522728@ntu.edu.tw, phone (+886)2-23620032; fax (+886)2-23641186

ABSTRACT

A high precision contact probe for a micro/nano-CMM was developed to detect the 3D motion of the stylus tip. This contact probe is composed of a stylus with a ball tip, a suspension plate and three displacement sensors. The stylus was connected to the suspension plate, which is suspended to the probe housing by three beryllium-copper leaf springs. A 3D translation of a ball tip causing by probing force would be transferred to three Z-displacements on the suspension plate. Displacement sensors, based on the classic model of Michelson interferometer, can measure nanoscale displacement on the plate. Calibrations with a nano measuring and positioning machine (NMM) proved the typical standard deviation was less than 20 nm for both the trigger and scanning modes.

Keywords: CMM, contact probe, suspension plate, Michelson interferometer

1. INTRODUCTION

There are more and more demands to measure the dimensions of tiny components with sub-micron or nanometer accuracy and uncertainty. Due to the development of nanotechnologies, the coordinate measuring machines (CMMs) are widely used to get the locations of measuring points. With software integrations it could be possible to detect the 3D dimensions of tiny structures. With the motion of the CMM, the probe or the work piece can get in touch with each other directly. At the same time, the PC-based controller will set the measuring contour according to the configurations of workpieces. As the CMM is getting smaller, the accuracy of the probe has a great effect on the whole uncertainty of the CMMs [1]. There are more and more researches on the development of high precision micro-CMM probes using various sensors, such as optical sensors [2], capacitance sensors [3], and piezo-resistive sensors [4].

Schellekens and Pril *et al* at the Eindhoven University of Technology [5] proposed a probe with piezo resistive strain gauges, which are fabricated on the three silicon slender rods using MEMS technologies. Displacement of the probe tip leads to elastic deformation of the entire suspension mechanism. This deformation would be measured by strain gauges. Thus, any direction of 3D translation on the probe tip would be detected and the suspension mechanism with a low moving mass of 25 mg has an isotropic stiffness of 480 N/m, that means the probe has equal sensitivity for every direction. The probe with a 300 μm diameter tip has 25 μm measuring range and 1 nm resolution.

Another typical probe is proposed by Gaoliang Dai *et al* at Physikalisch-Technische Bundesanstalt (PTB) in Germany [4]. The probe is composed of a boss membrane made from single crystalline silicon as suspension mechanism and four groups of strain gauges. When the probe tip gets in touch with measurement object, 3D displacement vector (dx, dy, and dz) of the probe tip would be transformed into a 4D signal vector. After calibration with NMM, they obtain a transition matrix (4 \times 3) which can convert the electrical signals into the displacement of the probe tip. The standard deviations of trigger points are 1.3 nm, 4.4 nm, 4.4 nm along the Z, Y and X direction. The stiffness along Z direction is deemed too high, about 3.65 kN/m, which is not suitable for long scanning range.

A new probe system for Micro-CMM is presented in this report. Rather than fabricating the structure by MEMS process, this probe can be made by conventional machining processes. In addition, three miniature linear interferometers are designed based on Michelson principle that can provide higher accuracy and resolution in sensing the stylus tip displacement.

2. DESIGN PRINCIPLES OF THE PROBE

A tactile contact probe should observe the demands of CMM metrology. The selection and design of the suspension mechanism and sensors would determine the final performance of the probe, which are [6]:

1. *High resolution.* The resolution means the minimum displacement sensors could detect. Michelson interferometers are known to have the best resolution down to less than one nanometer. The resolution of the sensor is directly proportional to the resolution of the probe.
2. *Miniature spherical tip.* The products of MEMS technology or micro-machining usually have micro-level characteristic dimensions. The probe tip is often used to insert into a gap or a hole to measure the groove profile. The smaller the ball tip is the smaller the groove can be measured.
3. *Low stiffness.* Due to the elastic deformation caused by the probing force, the measuring results would reveal wrong characteristic dimensions. In order to reduce this systematic error, the stiffness of the suspension mechanism should be as low as possible. The best probe is that the stiffness in all directions should be isotropic to compensate with equal values in the pre-travel distance of the probe.
4. *High natural frequency.* Because the effective damping coefficient of suspension mechanism is limited due to assembly considerations, the vertical vibration of suspensions would remain a minimal level. If the vibration is too serious, oscillations of the probe tip might affect the trigger point.

2.1 Michelson interferometers

The configuration of the new proposed optical system is illustrated in Fig. 1(a). A partially polarized laser beam of 635nm wavelength from the laser diode LD impinges on the polarizing beam splitter PBS1 and is split into two beams: the transmitted P-beam and the reflected S-beam. The left beam is reflected by the reference mirror M1, and the other one is reflected by the moving object mirror. The displacement of the object mirror will cause the optical path difference between the two reflected beams so as to produce interference. [7]

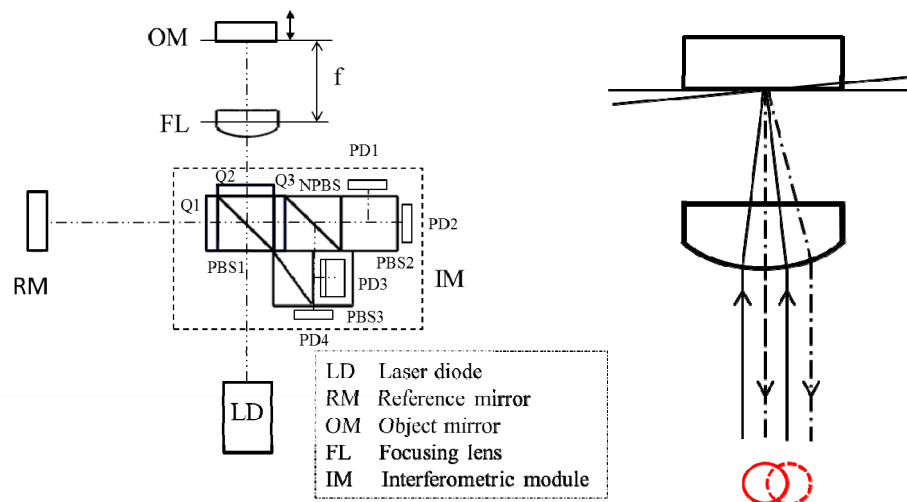


Figure 1. (a) The configuration of the Michelson interferometer (b)The spot movement when the object mirror is rotated

The quarter waveplates Q1 and Q2 prevent the reflected beams from going back into the laser diode, because each

polarization state will be changed by 90° after passing a quarter waveplate twice. The two reflected beams are combined at PBS1 and converted into left and right circularly polarized beams by Q3. With the phase shift module composed by NPBS, PBS2 and PBS3, the interference fringe with 90° phase shift can be detected by photo-detectors PD1 to PD4. Analyzed by Jones vector, the intensity of each photo-detector can be expressed as: [8]

$$I_{PD1} = A \left[1 - \cos\left(\frac{2\pi d}{\lambda}\right) \right] \quad (1)$$

$$I_{PD2} = A \left[1 + \cos\left(\frac{2\pi d}{\lambda}\right) \right] \quad (2)$$

$$I_{PD3} = A \left[1 + \sin\left(\frac{2\pi d}{\lambda}\right) \right] \quad (3)$$

$$I_{PD4} = A \left[1 - \sin\left(\frac{2\pi d}{\lambda}\right) \right] \quad (4)$$

Where, A and λ are the intensity and the wavelength of the laser beam, and d is the optical path difference of the two reflected beams. Fig. 1(b) shows the robustness of this system that even if the object mirror is tilted at a large angle θ the beam will be shift only with the amount of $2f\theta$, where f is the focal length of the focus lens. Without this special feature, the reflected beam will be shifted along the entire optical distance. The interfered beams will be separated causing low intensity.

2.2 The suspension mechanism

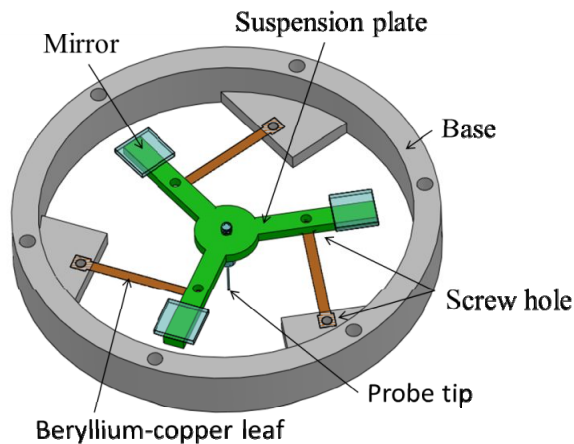


Figure 2. Schematic illustration of suspension mechanism

As shown in Fig. 2, the structure is composed of a stainless stylus with a fiber ball tip, a suspension plate, three beryllium-copper leaf springs and three mirrors attached on three measuring points. The stylus is screwed to the suspension plate. When a probing force is applied onto the ball tip, three leaf springs would give reaction forces to maintain forces and moments equilibrium. In order not to damage the work piece, the geometric characteristics of three leaf springs must ensure the trigger force being less than 1 mN. Additionally, the bending moments of three springs in probing processes are not permitted to exceed the elastic limit or the probe tip would be unable to return back to the initial position.

Another consideration about the suspension mechanism is the isotropic performance in all probing directions. An anisotropic suspension structure would result in “stick-slip effect” [9], which causes scanning result depending on the measuring direction, and the pretravel distance compensation would be more difficult in the software.

2.3 The probe system

Because a horizontal probing force would lead to an angle change of the suspension plate around X or Y axis, the sinusoid signals of the Michelson interferometer may get wrong values if the angle is too large. It is important to ensure all of three Michelson sensors reading correct values in the whole scanning range. The designed probe system is shown in Fig. 3. The ball tip displacement in Cartesian coordinate is related to the displacements of three mirrors, which are detected by three respective miniature linear interferometers. For the stability of probe signals, a special enclosure of the suspension plate and sensors would reduce external disturbances from acoustic vibration.

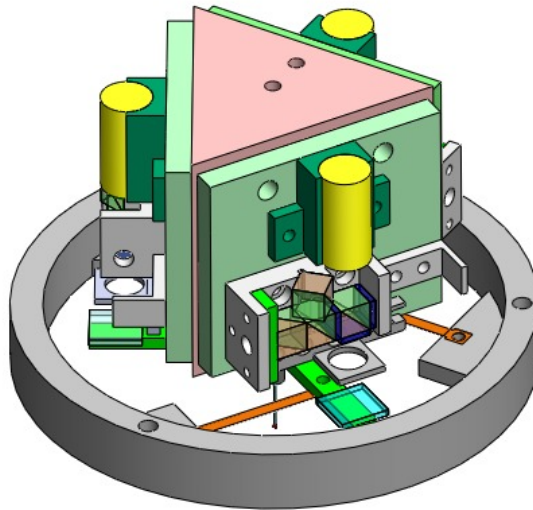


Figure 3. 3D structure of the probe

3. CALIBRATION OF THE PROBING SYSTEM

In order to establish metrological traceability, all of measuring instruments must be calibrated before using. Even though the Michelson sensors have been calibrated before assembling on the probe, the probe after assembly must be calibrated again due to the fact of non-symmetrical structure from fabrication and assembly errors. The most difficult challenge is to obtain the relationship between three Z-displacements on the suspension plate and the 3D displacement of the ball tip. In this research, a Nanopositioning and Measuring Machine (NMM), developed by SIOS Co., was used as the calibrator, which has very high accuracy. [10]

3.1 Transformation matrix

With a Taylor series expansion of the first order [11], the transformation matrix $\mathbf{T}_{3 \times 3}$ between three Michelson sensors and 3D displacement of the ball tip is represented in (5), where $\vec{U}_{3 \times 1}$ is a signal output vector of three Michelson interferometers, and $\vec{V}_{3 \times 1}$ is a vector of 3D displacement of the ball tip. It is difficult to obtain the matrix $\mathbf{T}_{3 \times 3}$ directly, however, we can get another matrix $\mathbf{S}_{3 \times 3}$, the inverse matrix of $\mathbf{T}_{3 \times 3}$ by calculating each slope of three Michelson interferometers individually in three independent directions.

$$\vec{V}_{3 \times 1} = \begin{pmatrix} \frac{\partial x}{\partial s_a} \\ \frac{\partial y}{\partial s_a} \\ \frac{\partial z}{\partial s_a} \end{pmatrix} = \begin{bmatrix} \frac{\partial x}{\partial s_a} & \frac{\partial x}{\partial s_b} & \frac{\partial x}{\partial s_c} \\ \frac{\partial y}{\partial s_a} & \frac{\partial y}{\partial s_b} & \frac{\partial y}{\partial s_c} \\ \frac{\partial z}{\partial s_a} & \frac{\partial z}{\partial s_b} & \frac{\partial z}{\partial s_c} \end{bmatrix} \begin{pmatrix} \delta s_a \\ \delta s_b \\ \delta s_c \end{pmatrix} = \mathbf{T}_{3 \times 3} \cdot \vec{U}_{3 \times 1} \quad (5)$$

3.2 Calibration

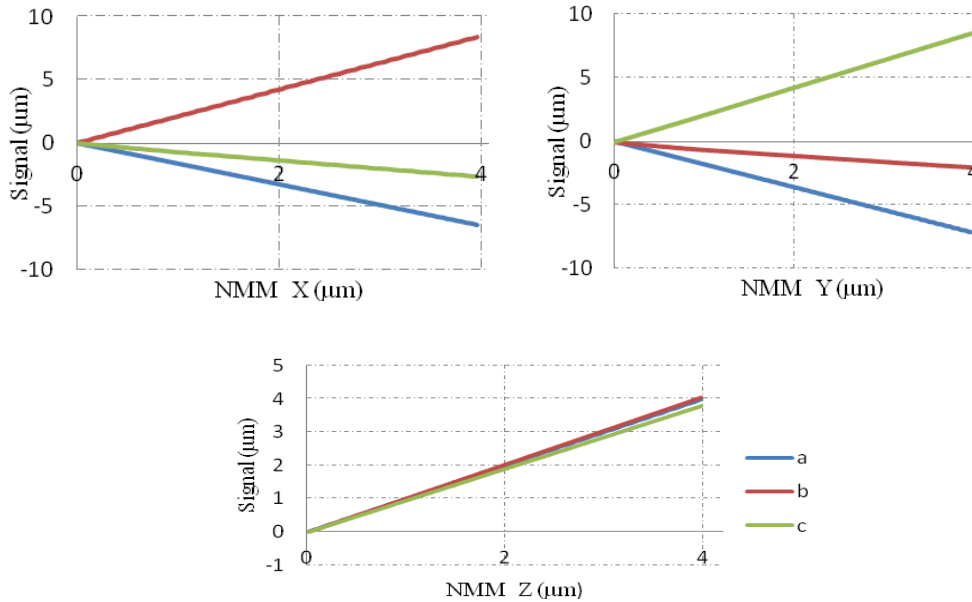


Figure 4. Probing sensitivity results with probing directions along the +X, +Y, +Z axes

After the probe is integrated with the NMM's controller both in hardware and software, a gauge block placed on the moving table NMM is used as the work piece to contact with the probe tip. Giving the probe tip with +X, +Y, and +Z displacements step by step, the slopes between three Michelson sensors and NMM position, as shown in Fig. 4, provide all nine elements in $S_{3 \times 3}$. After repeating the measurement at least 5 times the standard deviations of each direction reveal the scanning performance of this probe, as shown in (6) and Table 1.

$$S_{3 \times 3} = \begin{bmatrix} -1.631 & -1.8 & 1.002 \\ 2.138 & 0.437 & 1.014 \\ -0.651 & 2.161 & 0.951 \end{bmatrix} \quad (6)$$

Table 1. Sensitivity of three Michelson sensors to each directional motion of NMM

	Michelson A	Michelson B	Michelson C

Direction	AVG	STD/AVG	AVG	STD/AVG	AVG	STD/AVG
X	-1.631	0.001	2.138	0.002	-0.651	0.004
Y	-1.8	0.001	-0.473	0.01	2.161	0.001
Z	1.002	0.001	1.014	0.001	0.951	0.001

The transformation matrix $T_{3 \times 3}$ is then obtained by calculating the inverse matrix of $S_{3 \times 3}$.

$$T_{3 \times 3} = S^{-1}_{3 \times 3} = \begin{bmatrix} -0.196 & 0.2877 & -0.1003 \\ -0.1999 & -0.0667 & 0.2817 \\ 0.32 & 0.3485 & 0.3428 \end{bmatrix} \quad (7)$$

3.3 Scanning performance

The nine elements of the $T_{3 \times 3}$ are important parameters to this probe, with which we can convert three Michelson signals to 3D displacement of the probe tip. By using the transformation matrix $T_{3 \times 3}$, we can repeat the experiment of Figure 4.

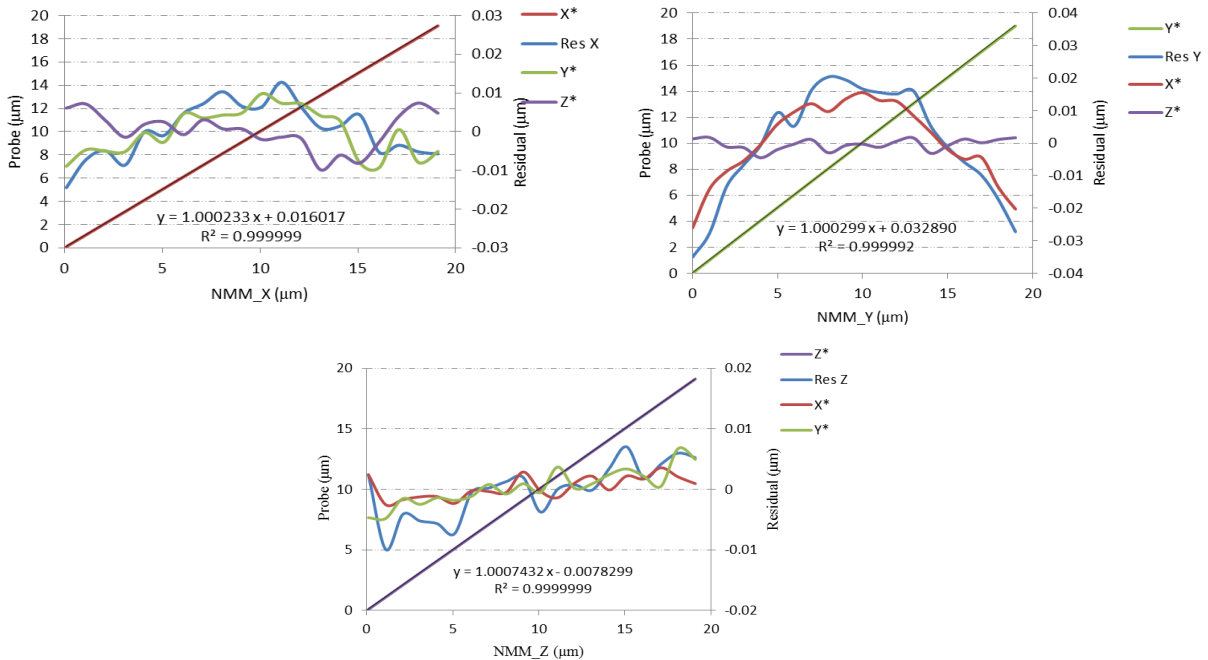


Figure 5. Probe outputs and residual along the X, Y and Z axes, respectively

As shown in Fig. 5, probe outputs by using the transformation matrix $T_{3 \times 3}$ have excellent linearity to the NMM stage positions that coefficients of determination R^2 are greater than 0.99999 over a 20 μm input displacement range. The

standard deviations of residuals in calibrated axes are 7 nm, 17 nm and 7 nm along the X, Y and Z axes, and the cross-talk residuals are less than 20 nm. This proves very good systematic accuracy of the probe system.

To verify the applicability of the transformation matrix $T_{3 \times 3}$ in different directions, the probe is measured along 45° direction in the XY plane. As shown in Fig. 6, the outputs of X and Y are nearly overlapped in 45° direction with a sensitivity difference about 0.0008 only. This result ensures the assumption of linear model and the transition matrix $T_{3 \times 3}$ is valid in any directions.

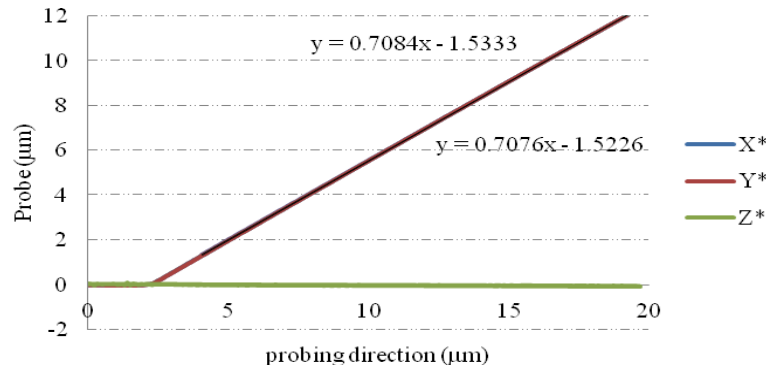


Figure 6. Probing along 45° direction

3.4 Trigger repeatability

A contact probe can be used in either scanning mode or trigger mode for different measurement demands. From experiments, it was found that the surface force between the probe tip and the object is apparent that significantly affects the trigger position, as shown in Fig. 7. This surface force is regarded as the attractive van der Waals' force in the near field within 1µm gap. In order not to be influenced by such a surface force, it is necessary to set a threshold to filter the data near the trigger point [12]. A least squares line fitting is carried out both before and after the contact and the intersection point is defined as the trigger point. The standard deviations of results are 5 nm, 3 nm and 11 nm along X, Y and Z axes, respectively.

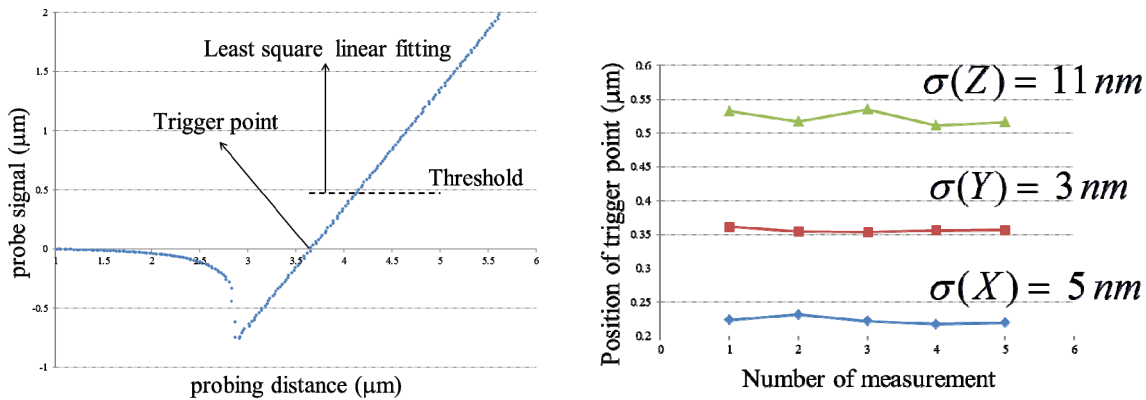


Figure 7. Probing curve and trigger repeatability

4. CONCLUSION

A new tactile probe for CMMs with high accuracy was developed and has been calibrated by NMM. Calibrations in X, Y and Z directions determine the transformation matrix and it is successful to verify this matrix in 45° direction. The probe is capable of measuring 3D displacement not only in calibrated axes. Its probing repeatability reaches 5 nm, 3nm and 11nm along the X, Y and Z axes, respectively.

ACKNOWLEDGEMENT

This work is sponsored by the National Science of Council of Taiwan under contract number NSC 100-2212-E-002-070-MY3,

REFERENCES

- [1] Takamasu, K., Ozawa, S., Asano, T., Suzuki, A., Furutani, R., Ozono, S., "Basic Concepts of Nano-CMM," The Japan - China Bilateral Symp. on Advanced Manufacturing Eng., 155-158 (1996).
- [2] Schwenke, H., Härtig, F., Wendt, K., Wäldele, F., "Future challenges in co-ordinate metrology: Address metrological problems for very small and very large parts," IDW 2001, 1-12 (2001).
- [3] Claverley, J. D., Leach, R. K., "A vibrating micro-scale CMM probe for measuring high aspect ratio structures," *Microsyst. Technol.*, vol. 16, 1507-1512 (2010).
- [4] Dai, G., Bütefisch, S., Pohlenz, F., Danzebrink, H.U., "A high precision micro/nano CMM using piezoresistive tactile probes," *Measurement Science and Technology*, 20, 084001-084009 (2009).
- [5] Haitjema, H., Pril, W. O., and Schellekens, P.H.J., "Development of a Silicon-based Nanoprobe System for 3-D Measurements," *CIRP Annals - Manufacturing Technology*, 365-368 (2001).
- [6] Pril, W. O., "Development of high precision mechanical probes for coordinate measuring machines," ISBN 90-386-2654-1, PhD thesis, Eindhoven University of Technology, Eindhoven, The Netherlands (2002).
- [7] Michelson, A. A., "On the Relative Motion of the Earth and the Luminiferous Ether," *American Journal of Science* 22, 120-129 (1881).
- [8] Cheng, F. and Fan, K. C., "Linear diffraction grating interferometer with high alignment tolerance and high accuracy," *Appl. Opt.* 50(22), 4550-4556 (2011).
- [9] Bos, E. J. C., Heldens, R. W. P., Delbressine, F. L. M., Schellekens, P. H. J., Dietzel, A., "Compensation of the anisotropic behavior of single crystalline silicon in a 3D tactile sensor," *Sens. Actuat. A* 134, 374-381 (2006).
- [10] Jäger, G., Manske, E., Hausotte, T., Büchner, H. J., "Nanomeasuring machines", *MICRO.tec 2000 Hannover*, 25-27 (2000).
- [11] Park, J.J., Kwon, K., Cho, N., "Development of a coordinate measuring machine (CMM) touch probe using a multi-axis force sensor", *Meas. Sci. Technol.* 17, 2380-2386 (2006)
- [12] Bos, E. J. C., "Aspect of tactile probing on the micro scale", *Precision Engineering* 35, 228-240 (2011)